Journal of Crystal Growth 401 (2014) 347–350

Contents lists available at ScienceDirect

Journal of Crystal Growth

journal homepage: www.elsevier.com/locate/jcrysgro

Modelling of X-ray diffraction curves for GaN nanowires on Si(1 1 1)

V.P. Kladko [a], A.V. Kuchuk [a,*], H.V. Stanchu [a], N.V. Safriuk [a], A.E. Belyaev [a], A. Wierzbicka [b], M. Sobanska [b], K. Klosek [b], Z.R. Zytkiewicz [b]

[a] V. Lashkaryov Institute of Semiconductor Physics, National Academy of Sciences of Ukraine, Pr. Nauky 41, 03028 Kyiv, Ukraine

[b] Institute of Physics, Polish Academy of Sciences, Al. Lotnikow 32/46, 02-668 Warsaw, Poland

ARTICLE INFO

Available online 28 January 2014

Keywords:
A1. High resolution X-ray diffraction
A1. Nanostructures
A1. Computer simulation
A3. Molecular beam epitaxy
B1. Nitrides
B2. Semiconducting III–V materials

ABSTRACT

X-ray diffraction curves and reciprocal space maps from self induced GaN nanowires on Si(1 1 1) substrates were examined theoretically and experimentally. Numerical simulation shows how distribution of such NWs parameters as diameter, length, strain and orientation influence broadening of X-ray diffraction peak profiles. Calculated shape of symmetric 0002 GaN reciprocal space map well correlates with experimental result, which indicates the validity of selected theoretical model.

1. Introduction

Recently the GaN nanowires (NWs) grown on various substrates have been extensively studied. At the same time many diagnostic methods are developed that allow analysis of NWs properties. For structural characterization the nondestructive X-ray diffraction (XRD) is mainly used.

The structure of GaN NWs, as well as of planar layers, is described by a model of mosaic crystal [1], which takes into account such parameters as tilt, twist and size of mosaic blocks (coherent length). All these parameters cause broadening of the X-ray diffraction profiles (XDP) for both types of epitaxial structures. However, there are strong differences between the full width at half maximum (FWHM) of XDPs of nanowire and planar GaN layers. For GaN layers the XDP broadening is caused mainly by different types of dislocations [2], while for dislocation-free GaN NWs broadening is caused by their small size as well as by large values of both in-plane (twist) and out-of-plane (tilt) angular distributions [3].

In most works the XRD is used mainly to determine the alignment of the GaN NWs with the substrate normal [4–6] or their polarity [7]. Recently [8], Jenichen et al. applied XRD for characterization macro- and micro-strain in GaN NWs on a Si(1 1 1) substrate. They also determined tilt, twist and size of NWs by X-ray φ-scans, reciprocal space map (RSM) and Williamson–Hall plots. However, only few works report on the influence of mosaicity parameters on the X-ray diffraction peak profiles from GaN NWs.

In [9], by using grazing-incidence XRD, the effect of mean GaN NWs diameter and its statistical distribution as well as influence of the root mean square twist on XDP broadening was studied. By comparing measured and fitted XDP a good correlation between the theoretical model and the experimental data has been shown. In [10], the theoretical study of the effect of inhomogeneous microstrains along the growth axis of GaN NWs on diffracted X-rays was presented. It was shown that an exponential decay of the mean-squared strain along the nanowire describes the peak profiles. The characteristic length of this decay is found to be about two times larger than the nanowire diameter. Thus, XDP and RSM modeling, and their comparison with experimental results allow to get the real structural parameters of the objects.

The purpose of this work is to develop a theoretical approach for calculation of the symmetric XDP of GaN NWs (in different directions relatively to the diffraction vector, so-called ω-, ω-2θ scans) taking into account various parameters, such as size, orientation, and their distribution functions. Then, XDP calculation with all these parameters taken into account would allow modeling of RSM from NWs ensemble.

2. Theoretical description

The kinematical scattering theory is applied to study XDP from NWs with aim to estimate their structural parameters, such as distribution of microstrain along the NW $\varepsilon(z)$, size and out-of-plane (σ_{tilt}) distributions. To simplify the theoretical calculation, we consider that NWs have a cylindrical shape with length L and radius R, whose form-factor is well-known and it is given by:

$$G(q_x, q_y, q_z) = \frac{\sin(2\pi q_z L)}{2\pi q_z L} \times \frac{J_1\left(2\pi R\sqrt{(q_x-\tilde{q}_x)^2+(q_y-\tilde{q}_y)^2}\right)}{2\pi R\sqrt{(q_x-\tilde{q}_x)^2+(q_y-\tilde{q}_y)^2}}, \quad (1)$$

where q_x, q_y, q_z—the components of diffraction vector; $\tilde{q}_x$, $\tilde{q}_y$—angular position of the analyzing crystal; $J_1(x)$—first order Bessel function.

* Corresponding author. Tel.: +380 66 158 8840; fax: +380 44 525 8342.
E-mail address: an.kuchuk@gmail.com (A.V. Kuchuk).

0022-0248/$ - see front matter © 2014 Elsevier B.V. All rights reserved.
http://dx.doi.org/10.1016/j.jcrysgro.2014.01.042

Usually the X-ray diffraction profile (XDP) of GaN NWs cannot be described by using distribution function of only one mosaicity parameter. We suppose that different structural parameters have different influence on each part of XDP. The broadening of rocking curves (ω-scan) of the symmetric reflections is influenced only by the tilt and diameter (D) of NWs. To describe tilt and D distribution of GaN NWs the Gaussian (Eq. (2)) and asymmetrical gamma (Eq. (3)) functions were chosen, respectively [11,12].

$$f(q_x, q_y) = \frac{1}{\sqrt{2\pi}\sigma_h}\exp\left(-\frac{q_x^2+q_y^2}{2\sigma_h^2}\right), \tag{2}$$

where σ_h—dispersion parameter of distribution.

$$\gamma(t(r,R),N) = \frac{t^{N-1}e^{\frac{-t}{2}}}{2^N\Gamma(N)}, \tag{3}$$

where $t(r,R) = 2(N-1)r/R$; Γ(N)—gamma function.

X-ray scattering functions with the form-factor (Eq. (1)) and distributions (Eqs. (2) and (3)) were given by:

$$I_s(q_x, q_y, q_z) = C \times \int_0^{\infty} G^2(q_x, q_y, q_z) \times \gamma(t(r,R),N)dr, \tag{4}$$

$$I_{or}(q_x, q_y, q_z) = C \times \int_{-\infty}^{\infty}\int_{-\infty}^{\infty}\int_{-\infty}^{\infty} G^2(q_x-\tilde{q}_x, q_y-\tilde{q}_y, q_z) \times f(\tilde{q}_x, \tilde{q}_y)dq_y d\tilde{q}_x d\tilde{q}_y, \tag{5}$$

where C—constant; I_s, I_{or}—intensity distributions where only nanowire size or orientation is taken into account, respectively.

The length and microstrain distributions along the c-axis of NWs cause a broadening of symmetric $\omega-2\theta$ diffraction peaks. The NWs length contribution on broadening of symmetric $\omega-2\theta$ diffraction peaks is given by:

$$I(q_z) = \frac{\sin^2(2\pi q_z L)}{(2\pi q_z L)^2}, \tag{6}$$

It is evident that microstrain is not uniformly distributed along the NWs length, because of strain relaxation at their side walls. Therefore, an important issue to study is the evolution of microstrain along NWs. According to [13], the intensity distribution in the direction of diffraction vector can be written as:

$$I(q_z) = \int_0^L \frac{dz}{\varepsilon(z)}\exp\left(-\frac{1}{2}\left(\frac{q_z}{\varepsilon(z)Q}\right)\right), \tag{7}$$

where $\varepsilon(z) = \varepsilon_o L/z$; ε_o—describes the minimum strain fluctuations in the nanowire and Q is the reciprocal lattice vector.

3. Experiment

Self-induced GaN NWs were grown by plasma-assisted molecular beam epitaxy on Si(1 1 1) substrate at ~760 °C under highly nitrogen-rich conditions. Before the growth started, the substrate was exposed to a nitrogen flux for 30 min at the nitridation temperature ~450 °C (see [14] for details).

The samples were examined *ex-situ* by using a scanning electron microscope (SEM) Hitachi SU-70 and high-resolution X-ray diffraction (XRD) PANalytical X'Pert Pro MRD XL. We used a standard four-bounce Ge(2 2 0) monochromator and three bounce (0 2 2) channel cut Ge analyzer crystal as well as 1.6 kW X-ray tube with Cu$K\alpha_1$ radiation and vertical line focus. The symmetric 0002, 0004, and 0006 GaN reflections were measured by ω and $\omega-2\theta$ Bragg scans. Finally, the symmetric RSM around the 0002 GaN reflection was measured.

4. Results and discussion

The theory described above was used for the calculation of ω and $\omega-2\theta$ scans of the 0002 reflection from GaN NWs. Fig. 1(a) shows X-ray diffraction profiles calculated for constant tilt value (1°) and diameters varied from 10 nm to 80 nm. It is visible that ω-scans

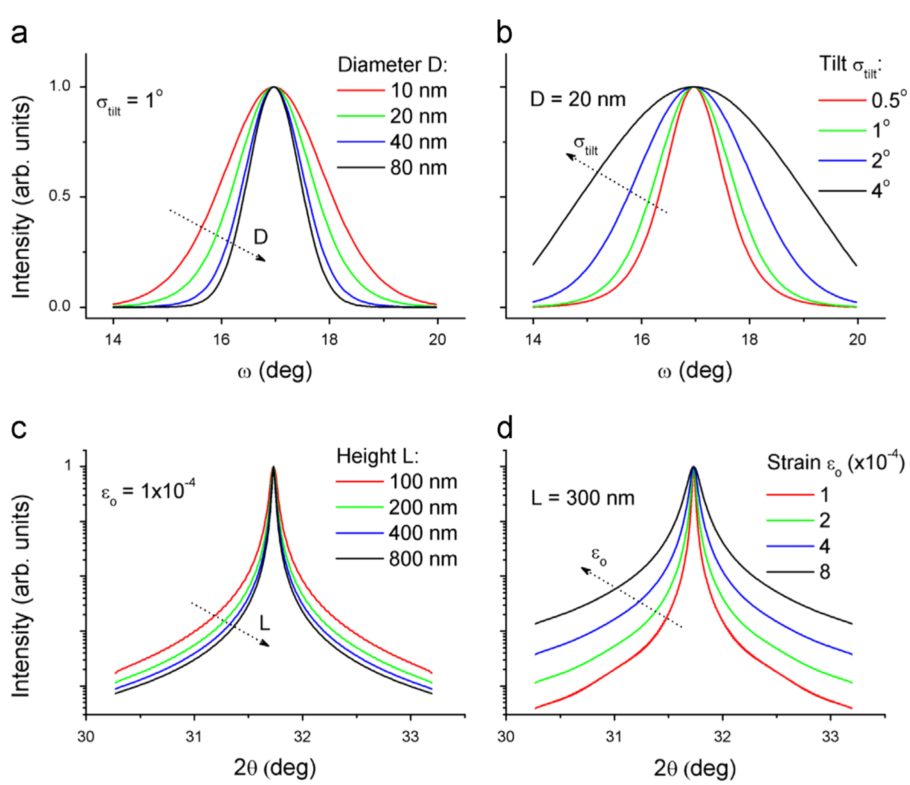

Fig. 1. X-ray diffraction profiles of ω and $\omega-2\theta$ scans of the symmetric 0002 GaN reflection from GaN NWs with different structural parameters: (a) diameter; (b) tilt; (c) length and (d) strain.

become broader when diameter of NWs decreases. The obvious situation is presented on Fig. 1(b) where the larger tilt value causes the broadening of XDP. In order to obtain information about the length and distribution of microstrain along NWs we calculated $\omega-2\theta$-scans. For the constant strain value ($\varepsilon_o=1\times10^{-4}$) the diffraction curve from longer NWs is narrower and has smaller contribution to the tails of the curve (Fig. 1(c)). If the microstrain along the NWs increases (when the length of NW is constant) we get broader XDP and the contribution to the tails of the diffraction curve is bigger (Fig. 1(d)).

The contribution of each described parameter of GaN NWs into the shape of XDP is shown in Fig. 2. Fig. 2(a) presents the XDPs with the NWs parameters of only diameter (red solid line calculated by Eq. (4)) and only tilt (black dashed line calculated by Eq. (5)) distribution plotted together to estimate their contribution to the common XDP. As can be seen from Fig. 2(a), the NWs diameters provide a larger contribution on the tails of XDP, whereas the broadening near the Bragg position is mainly caused by tilt distribution. In the same way, by using Eqs. (6) and (7), we estimate the contribution of the length and strain distribution of GaN NWs to the common XDP (Fig. 2(b)). In this case, the broadening of XDP in a large angular range is mainly caused by microstrain along the NWs *c*-axis. The NWs vertical size prevails only near the Bragg position.

Fig. 3(a) and (b) show experimental and calculated diffraction curves (ω and $\omega-2\theta$ scans) of symmetrical 0002 GaN reflection from NWs ensemble. The average parameters obtained from the XDP simulations are as follows: the tilt angle $\sigma_{\text{tilt}}=0.9^\circ$, length $L=300$ nm and the microstrain along *c*-axis $\varepsilon_o=1.8\times10^{-4}$. Moreover, from SEM analysis (insert on Fig. 3(a)) the distribution of NWs diameters is obtained. The best fit to SEM data with the same average value of D ≈ 30 nm was obtained also by the XDP calculation of ω scan. Next, measuring in triple-axis geometry 0002, 0004 and 0006 GaN diffraction curves, the Williamson–Hall (WH) plots were prepared (Fig. 4(a) and (b)). The details of WH plot analysis can be found elsewhere [15,16]. The fitting of linear function to experimental points on WH plots allows to determine the mosaicity parameters of GaN NWs, mentioned above. This procedure gave the following average values of the tilt $\sigma_{\text{tilt}}=1.2^\circ$, the length $L=274$ nm, the microstrain along *c*-axis $\varepsilon_o=1\times10^{-4}$ and the NWs diameter $D=35.4$ nm. There is a good correlation between parameters, obtained from WH analysis and simulation of XDPs. However, while WH plots give average values of mosaicity parameters, the calculation of XDPs allows to obtain the distribution function of these parameters.

The agreement of calculations and experiment results is very good indicating correctness of the model used for XDP calculations. In the next step, we calculated the two-dimensional intensity distribution (RSM) in reciprocal space for symmetric GaN 0002 reflection. Fig. 5 (a) and (b) show the simulated and experimental RSM for GaN NWs around (0 0 0 2) reflection. To calculate the RSM, we used parameters ($\sigma_{\text{tilt}}=0.9^\circ$, $D=29$ nm, $\varepsilon_o=1.8\times10^{-4}$, $L=300$ nm) obtained by simulation of ω and $\omega-2\theta$ scans. With the aim to simplify the calculation, we assumed the linearity of the ω-scan. A good agreement of calculated and experimental RSMs can be seen. This indicates the accuracy and adequacy of the model, selected for the calculation of the

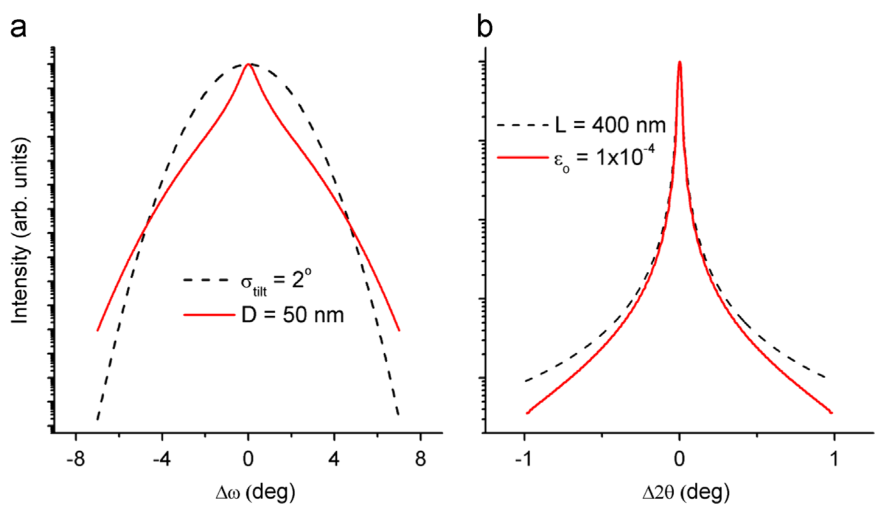

Fig. 2. The XDPs with contribution of GaN NWs parameters: (a) tilt and diameter; (b) length and strain.

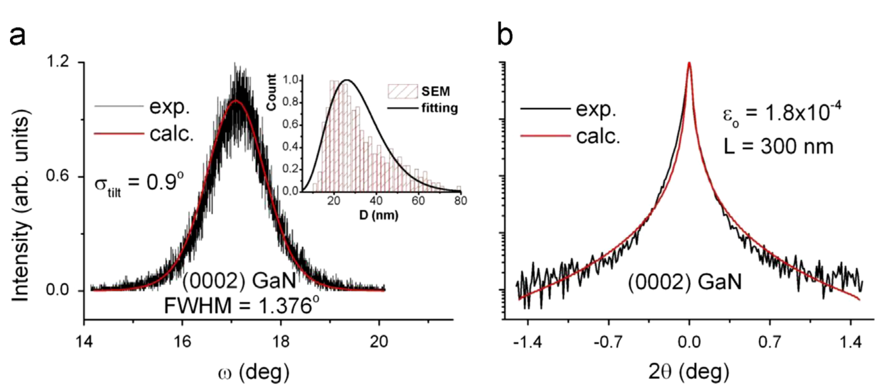

Fig. 3. The XDPs of measured and calculated ω (a) and $\omega-2\theta$ (b) scans of the symmetric Bragg reflection 0002 GaN. The insert presents the NWs diameter distribution from SEM image and curve calculated from XRD data.

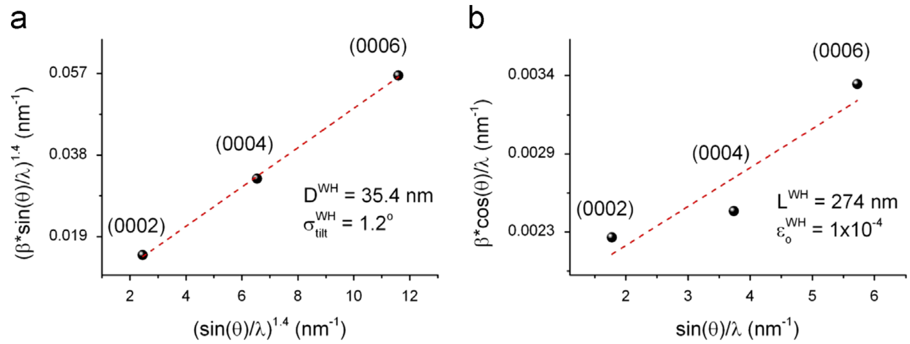

Fig. 4. The Williamson–Hall plots for the symmetrical GaN reflections.

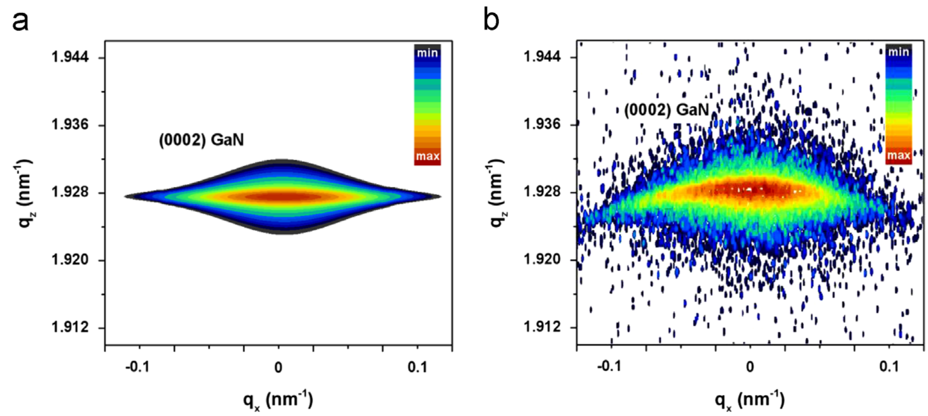

Fig. 5. Calculated (a) and experimental (b) reciprocal space map of 0002 GaN reflection.

intensity angular dependence for different directions, relative to the diffraction vector. Analyzing the shape of RSMs and the parameters obtained from simulation, we can conclude, that their elongated shape is caused mostly by wide tilt distribution of GaN NWs.

5. Conclusion

In this paper a theoretical analysis of the distributions of X-ray intensity around the symmetrical reciprocal lattice nodes from NW ensemble were studied. Theoretical expressions were adapted for the analysis of ω and $\omega-2\theta$ XDPs, measured in the triple axis mode. It was shown that the XDPs are very sensitive to the distribution of such NWs parameters as their lateral and vertical size, in-plane and out-of-plane orientation, and strain state. It was shown, how the different contribution of quoted parameters affects the XDP. It was found, that the size (length and diameter) of NWs significantly contributes to the width of diffraction curve on its tails, while the tilt and strain dominate in the curve broadening at the angles near the exact Bragg position. The parameters obtained by XDP simulation are in good agreement with those received by Williamson–Hall plots and SEM data. Thus, the modeling procedure presented in this work allows accurate determination of structural parameters of nanowires from simple XRD data.

Acknowledgments

This work was partly supported by the European Union within European Regional Development Fund, through grant Innovative Economy (POIG.01.01.02-00-008/08 NanoBiom) and by scientific-technological program “Nanotechnology and Nanomaterials” of the National Academy of Sciences of Ukraine.

References

[1] X.J. Ning, F.R. Chien, P. Pirouz, J.W. Wang, M.A. Khan, J. Mater. Res. 3 (1996) 580.
[2] S.R. Lee, P.P. Provencio, D.D. Koleske, A.M. West, A.A. Allerman, K.E. Waldrip, D.M. Follstaedt, Appl. Phys. Lett. 86 (2005) 241904.
[3] F. Furtmayr, M. Vielemeyer, M. Stutzmann, J. Arbiol, S. Estradé, F. Peirò, J. Ramon Morante, M. Eickhoff, J. Appl. Phys. 104 (2008) 034309.
[4] L. Largeau, D.L. Dheeraj, M. Tchernycheva, G.E. Cirlin, J.C. Harmand, Nanotechnology 19 (2008) 155704.
[5] K.A. Bertness, A. Roshko, L.M. Mansfield, T.E. Harvey, N.A. Sanford, J. Cryst. Growth 310 (2008) 3154–3158.
[6] L. Geelhaar, C. Ch'eze, B. Jenichen, IEEE J. Sel. Top. Quantum Electron. 17 (2011) 4.
[7] K. Hestroffer, C. Leclere, C. Bougerol, H. Renevier, B. Daudin, Phys. Rev. 84 (2011) 245302.
[8] B. Jenichen, O. Brandt, C. Pfüller, P. Dogan, M. Knelangen, A. Trampert, Nanotechnology 22 (2011) 295714.
[9] L. Horák, V. Holý, C.R. Staddon, N.R.S. Farley, S.V. Novikov, R.P. Campion, C.T. Foxon, J. Appl. Phys. 104 (2008) 103504.
[10] V.M. Kaganer, B. Jenichen, O. Brandt, S. Fernandez-Garrido, P. Dogan, L. Geelhaar, H. Riechert, Phys. Rev. B: Condens. Matter 86 (2012) 115232.
[11] V.S. Harutynyan, E. Zielinska-Rohozinska, M. Regulska, J. Alloys Compd. 362 (2010) 287.
[12] T. Kawamura, S. Bhunia, Y. Watanabe, S. Fujikawa, J. Matsui, Y. Kagoshima, Y. Tsusaka, J. Appl. Phys. 97 (2005) 084318.
[13] V.M. Kaganer, M. Ẅolz, O. Brandt, L. Geelhaar, H. Riechert, Phys. Rev. B: Condens. Matter 83 (2011) 245321.
[14] A Wierzbicka, Z.R. Zytkiewicz, S. Kret, J. Borysiuk, P. Dluzewski, M. Sobanska, K. Klosek, A. Reszka, G. Tchutchulashvili, A. Cabaj, E. Lusakowska, Nanotechnology 24 (2013) 035703.
[15] G.K. Williamson, W.H. Hall, Acta Metall. 1 (1953) 22–31.
[16] E. Dimakis, J.Z Domagala, A. Delimitis, Ph. Komniou, A. Adikimenakis, E. Iliopoulos, A. Georgakilas, Superlattices Microstruct. 40 (2006) 246–252.